Mon. Not. R. Astron. Soc. **325,** 989–994 (2001)

General relativistic spectra of accretion discs around rapidly rotating neutron stars: effect of light bending

Sudip Bhattacharyya,[1,2]★ Dipankar Bhattacharya[3]★ and Arun V. Thampan[4]★

[1]*Joint Astronomy Program, Indian Institute of Science, Bangalore 560012, India*
[2]*Indian Institute of Astrophysics, Bangalore 560034, India*
[3]*Raman Research Institute, Bangalore 560012, India*
[4]*Inter-University Centre for Astronomy and Astrophysics, Pune 411007, India*

Accepted 2001 February 21. Received 2001 February 21; in original form 2000 October 12

ABSTRACT

We present computed spectra, as seen by a distant observer, from the accretion disc around a rapidly rotating neutron star. Our calculations are carried out in a fully general relativistic framework, with an exact treatment of rotation. We take into account the Doppler shift, gravitational redshift and light-bending effects in order to compute the observed spectrum. We find that light bending significantly modifies the high-energy part of the spectrum. Computed spectra for slowly rotating neutron stars are also presented. These results would be important for modelling the observed X-ray spectra of low-mass X-ray binaries containing fast-spinning neutron stars.

Key words: accretion, accretion discs – relativity – stars: neutron – stars: rotation – X-rays: binaries.

1 INTRODUCTION

The central accretors in a large number of low-mass X-ray binaries (LMXBs) are believed to be neutron stars, rotating rapidly due to accretion-induced angular momentum transfer. LMXBs are thought to be the progenitors of millisecond (ms) radio pulsars (Bhattacharya & van den Heuvel 1991) like PSR 1937+21 with $P \sim 1.56$ ms (Backer et al. 1982). The recent discovery of millisecond ($P \sim 2.49$ ms) X-ray pulsations in XTE J1808−369 (Wijnands & van der Klis 1998) has strengthened this hypothesis. Kilohertz quasi-periodic oscillations (kHz QPOs) seen in a number of LMXBs are another indicator of the rapid rotation of the accreting neutron star. For example, in beat-frequency models of kHz QPOs, the difference (∼300–500 Hz) in the frequencies of two simultaneously observed kHz QPO peaks is interpreted as the rotational frequency of the neutron star (e.g. van der Klis 2000).

Fast rotation makes the neutron star considerably oblate and also modifies both the interior and the exterior space–time geometry. These, in turn, modify the size and the temperature profile of the accretion disc and hence the corresponding spectrum (Bhattacharyya et al. 2000; Bhattacharyya, Misra & Thampan 2001). General relativity also plays an important role in shaping the spectrum. As neutron stars are very compact objects, the effect of general relativity is very significant, particularly near the surface of the star.

For luminous LMXBs, the observed X-ray spectrum can be well fitted by the sum of a multicolour blackbody spectrum (presumably from the accretion disc) and a single-temperature blackbody spectrum (presumably from the boundary layer) (see Mitsuda et al. 1984). The multicolour spectrum can be calculated if the temperature profile in the accretion disc is known. Recently Bhattacharyya et al. (2000) have calculated the disc temperature profile as a function of the spin rate (Ω) and the mass (M) of the neutron star for different equations of state (EOS), including the effects of rotation and general relativity. In this paper, we calculate the observed spectrum from the accretion disc, using the temperature profiles. While doing so, we take into account the effects of gravitational redshift, Doppler broadening and the light-bending effect in the gravitational field of the accreting star.

For non-rotating neutron stars, an attempt has been made by Ebisawa, Mitsuda & Hanawa (1991) to compute the disc spectrum including the effects mentioned above. Sun & Malkan (1989) included relativistic effects of disc inclination, including Doppler boosting, gravitational focusing, and gravitational redshift, on the observed disc spectra for both Kerr and Schwarzschild black holes (in the context of supermassive black holes). They find (as we also do) that the higher energy part of the spectrum gets significantly modified due to the general relativisitic effects. A computation similar to that of Ebisawa et al. (1991), for Galactic black hole candidates, has been done by Asaoka (1989) using the Kerr metric. However, our work incorporating both the full general relativistic effects of rapid rotation, and the realistic EOS describing interiors of neutron stars, using an appropriate metric, is the first calculation for rotating neutron stars. In the present work we ignore the effects of the stellar magnetic field, so our results are applicable to weakly magnetized neutron stars.

The structure of the paper is as follows. In Section 2, we describe

★E-mail: sudip@physics.iisc.ernet.in (SB); dipankar@rri.res.in (DB); arun@iucaa.ernet.in (AVT)

a framework for the calculation of neutron star structure, disc temperature profile and observed spectrum. We also comment here on the chosen EOS. We describe the numerical procedure for spectrum calculation in Section 3. The results of the spectrum calculation are displayed in Section 4. We summarize the conclusions in Section 5 and list some relevant mathematical expressions in the Appendix.

2 THEORY

2.1 Neutron star structure calculation

We calculate the structure of a rapidly rotating neutron star for realistic EOS models, using the same procedure as adopted by Cook, Shapiro & Teukolsky (1994) (see also Datta et al. 1998). With the assumption that the star is rigidly rotating and a perfect fluid, we take a stationary, axisymmetric, asymptotically flat and reflection-symmetric (about the equatorial plane) metric, given by

$$\begin{aligned} \mathrm{d}S^2 &= g_{\mu\nu}\,\mathrm{d}x^{\mu}\mathrm{d}x^{\nu}(\mu,\nu=0,1,2,3) \\ &= -\,\mathrm{e}^{\gamma+\rho}\,\mathrm{d}t^2+\mathrm{e}^{2\alpha}(\mathrm{d}\bar{r}^2+\bar{r}^2\,\mathrm{d}\theta^2) \\ &\quad +\,\mathrm{e}^{\gamma-\rho}\bar{r}^2\sin^2\theta(\mathrm{d}\phi-\omega\,\mathrm{d}t)^2 \end{aligned} \tag{1}$$

where the metric potentials γ, ρ, α and the angular speed ω of the zero-angular-momentum observer (ZAMO) with respect to infinity are all functions of the quasi-isotropic radial coordinate ($\bar{r}$) and polar angle (θ). The quantity $\bar{r}$ is related to the Schwarzschild-like radial coordinate (r) by the equation $r=\bar{r}\,\mathrm{e}^{(\gamma-\rho)/2}$. We use the geometric units $c=G=1$ in this paper.

We solve Einstein's field equations and the equation of hydrostatic equilibrium self-consistently and numerically from the centre of the star up to infinity to obtain γ, ρ, α, ω and Ω (angular speed of neutron star with respect to infinity) as functions of $\bar{r}$ and θ. This is done for a particular EOS, assumed values of central density, and ratio of polar to equatorial radii. The obtained numerical equilibrium solutions of the metric enable us to calculate bulk-structure parameters, such as gravitational mass (M), equatorial radius (R), and angular momentum (J) of the neutron star. We also calculate the radius ($r_{\rm orb}$) of the innermost stable circular orbit (ISCO), specific energy ($\tilde{E}$) and specific angular momentum ($\tilde{l}$) of a test particle in a Keplerian orbit and the Keplerian angular speed ($\Omega_{\rm K}$) (see Thampan & Datta 1998 for a detailed description of the method of calculation).

2.2 Equation of state

The neutron star structure parameters are sensitive to the chosen EOS. In the literature, there exist a large number of EOSs ranging from very soft ones to very stiff ones. For the purpose of a general study, we have chosen four EOSs, of which one is soft [EOS:A, Pandharipande (1971) (hyperons)], one is intermediate [EOS:B, Baldo, Bombaci & Burgio (1997) (AV14+3bf)] in stiffness and the other two are stiff [EOS:C, Walecka (1974) and EOS:D, Sahu, Basu & Datta (1993)]. Of these EOSs, D is the stiffest.

The structure of a neutron star for a given EOS is described uniquely by two parameters: the gravitational mass (M) and the angular speed (Ω). For each chosen EOS, we construct constant-M equilibrium sequences with Ω varying from the non-rotating case up to the centrifugal mass-shed limit (rotation rate at which inwardly directed gravitational forces are balanced by outwardly directed centrifugal forces). Depending on Ω, M and the EOS model, neutron stars may have $R > r_{\rm orb}$ or $R < r_{\rm orb}$.

2.3 Disc temperature profile calculation

The effective temperature of a thin blackbody disc is given by

$$T_{\rm eff}(r)=[F(r)/\sigma]^{1/4} \tag{2}$$

where σ is the Stefan–Boltzmann constant and F is the X-ray energy flux per unit surface area. We calculate F using the expression of Page & Thorne (1974) (valid for a geometrically thin, non-self-gravitating disc embedded in a general axisymmetric space–time) for the accretion disc around a rotating black hole as

$$F(r)=\frac{\dot{M}}{4\pi r}f(r) \tag{3}$$

where

$$f(r)=-\Omega_{{\rm K},r}(\tilde{E}-\Omega_{\rm K}\tilde{l})^{-2}\int_{r_{\rm in}}^{r}(\tilde{E}-\Omega_{\rm K}\tilde{l})\tilde{l}_{,r}\,\mathrm{d}r. \tag{4}$$

Here $r_{\rm in}$ is the disc inner edge radius and a comma followed by a variable as subscript to a quantity represents a derivative of the quantity with respect to the variable.

Bhattacharyya et al. (2000) argue that, although formulated for the case of black holes, these expressions hold quite well for the case of neutron stars also. If $R > r_{\rm orb}$, then the disc will touch the star and we take $r_{\rm in}=R$. Otherwise, $r_{\rm in}=r_{\rm orb}$.

The temperature profile of the accretion disc, calculated as described in this and the previous subsections, is a function of M and Ω of the central star for any adopted EOS.

2.4 Calculation of the spectrum

To calculate the disc spectrum in full general relativity including the light-bending effect for rapid rotation we adopt the following procedure.

The observed spectrum from the accretion disc is given by

$$F(E_{\rm ob})=(1/E_{\rm ob})\int I_{\rm ob}(E_{\rm ob})\,\mathrm{d}\Pi_{\rm ob} \tag{5}$$

where the subscript 'ob' denotes the quantity in the frame of the observer, F is expressed in photon $\mathrm{s}^{-1}\,\mathrm{cm}^{-2}\,\mathrm{keV}^{-1}$, E is the photon energy in keV, I is the specific intensity and Π is the solid angle subtended by the source at the observer.

As I/E^3 remains unchanged along the path of a photon (Misner, Thorne & Wheeler 1973), it is possible to calculate $I_{\rm ob}$ if $I_{\rm em}$ is known. (We use the subscript 'em' to denote the quantities in the frame of the emitter.) We assume the accretion disc to radiate like a diluted blackbody (see Shimura & Takahara 1995). So $I_{\rm em}$ is given by

$$I_{\rm em}=(1/f^4)B(E_{\rm em},T_{\rm c}) \tag{6}$$

where f is the colour factor of the disc, B is the Planck function and $T_{\rm c}=fT_{\rm eff}$.

The quantities $E_{\rm ob}$ and $E_{\rm em}$ are related by $E_{\rm em}=E_{\rm ob}(1+z)$, where $(1+z)$ contains the effects of both gravitational redshift and Doppler shift. $(1+z)$ is given by (Luminet 1979)

$$1+z=(1+\Omega_{\rm K}b\sin\alpha\sin i)(-g_{tt}-2\Omega_{\rm K}g_{t\phi}-\Omega_{\rm K}^2g_{\phi\phi})^{-1/2} \tag{7}$$

where i is the inclination angle of the disc with respect to an observer at infinity, b is the impact parameter of the photon relative to the line joining the source and the observer and α is the polar angle of the position of the photon on the photographic plate of the observer. Therefore $b\,\mathrm{d}b\,\mathrm{d}\alpha$ is the apparent area of a disc element in

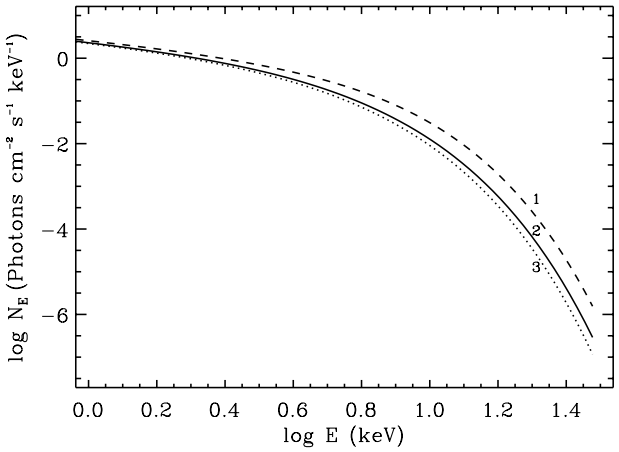

Figure 1. Effect of general relativity: spectra from an accretion disc around a neutron star of mass $1.4\,M_\odot$. All the curves are for EOS model (B), $\Omega = 0$, $D = 5$ kpc, $i = 60°$, $\dot{M} = 10^{18}\,g\,s^{-1}$ and $f = 2$. Curve (1) corresponds to the Newtonian case, curve (2) to the general relativistic case including the effect of light bending, and curve (3) to the general relativistic case without considering the effect of light bending.

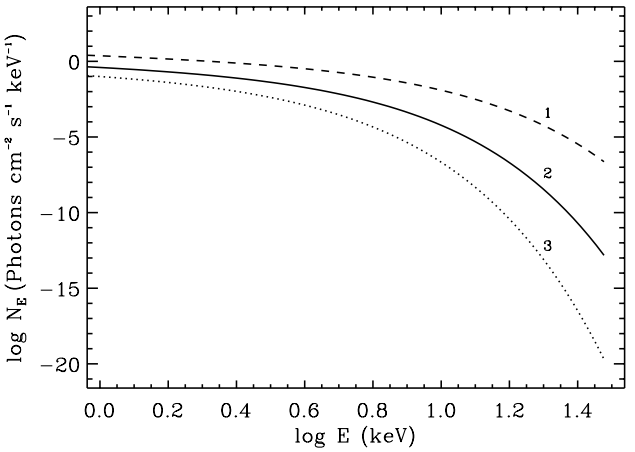

Figure 2. Accretion rate dependence: general relativistic spectra including light-bending effects from an accretion disc around a neutron star of mass-shed limit configuration ($\Omega = 7001\,rad\,s^{-1}$). Curve (1) corresponds to $\dot{M} = 10^{18}\,g\,s^{-1}$, curve (2) to $\dot{M} = 10^{17}\,g\,s^{-1}$ and curve (3) to $\dot{M} = 2 \times 10^{16}\,g\,s^{-1}$. The values of all the other parameters are as given in Fig. 1.

the sky of the observer and the corresponding solid angle is given by

$$d\Pi_{ob} = \frac{b\,db\,d\alpha}{D^2} \tag{8}$$

where D is the distance of the source from the observer.

3 NUMERICAL PROCEDURE

For a configuration, described by M and Ω (and thus specified by a set of $g_{\mu\nu}$), we obtain Ω_K. To calculate the spectrum for a given value of i with light-bending effects, we backtrack the path of the photons from the observer to the disc, using standard ray-tracing techniques (e.g. Chandrasekhar 1983) and the relevant boundary conditions. For the metric equation (1) that we use, the EOSs for photons are provided in the Appendix. We cover the disc between the radii r_{in} and $r_{mid} = 1000 r_g$; r_{in} being the radius of the inner edge of the disc and r_g the Schwarzschild radius. (Increasing r_{mid} has no significant effect on the spectrum.) Beyond r_{mid}, we ignore the effect of light bending, i.e. we take $b \sin\alpha = r \sin\phi$ (ϕ is the azimuthal angle on the disc plane) and $d\Pi_{ob} = (r\,dr\,d\phi \cos i)/D^2$ (Bhattacharyya et al. 2001).

We have performed several consistency checks on our results. (1) By switching off the light-bending effect (i.e. by considering flat space–time while backtracking the path of the photon), we see that the spectrum matches very well with that computed by ignoring light-bending effects (calculated by an independent code – Bhattacharyya et al. 2001). Also, in this case, the analytically calculated values of several quantities on the disc plane (e.g. r, ϕ, $d\phi/dt$, $d\theta/dt$ etc.) are reproduced satisfactorily by our numerical method. (2) An increase in the number of grid points on the (b, α) plane does not have any significant effect on the computed spectrum. (3) The spectrum matches very well with the Newtonian spectrum (Mitsuda et al. 1984) at the low-energy limit. This would imply that for higher frequencies, our spectrum is correct to within 0.2 to 0.3 per cent.

4 RESULTS

We calculate the general relativistic spectrum from the accretion disc around a rapidly rotating neutron star, taking into account the light-bending effect. The spectrum is calculated as a function of six parameters: M, Ω, D, i (for face-on, $i = 0°$), $\dot{M}$ and f, for each of the chosen EOSs. Our results are displayed in Figs 1–5. In all the displayed spectra, we have assumed $M = 1.4\,M_\odot$ (canonical mass for neutron stars), $D = 5$ kpc and $f = 2.0$.

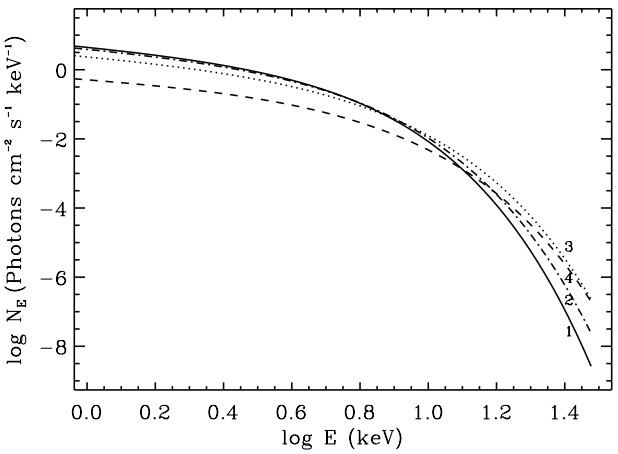

Figure 3. Inclination angle dependence: general relativistic spectra including light-bending effects from an accretion disc around a neutron star of mass-shed limit configuration ($\Omega = 7001\,rad\,s^{-1}$). Curve (1) corresponds to $i = 0°$, curve (2) to $i = 30°$, curve (3) to $i = 60°$ and curve (4) to $i = 85°$. The values of all the other parameters are as given in Fig. 1.

In Fig. 1, we have plotted the Newtonian spectrum and general relativistic (GR) spectra with (LBGR) and without (NLBGR) light-bending effects, keeping the same values for all the parameters. At 10 keV, the Newtonian flux is almost 2.5 times the LBGR flux. This is expected, because in the inner parts of the disc, the Newtonian temperature is considerably higher than the GR temperature (see fig. 2 of Bhattacharyya et al. 2000). The LBGR flux is about 50 per cent higher than the NLBGR flux at 10 keV. This is because light bending causes the disc to subtend a larger solid angle at the observer than otherwise. Thus, the general effect of light bending is to increase the observed flux.

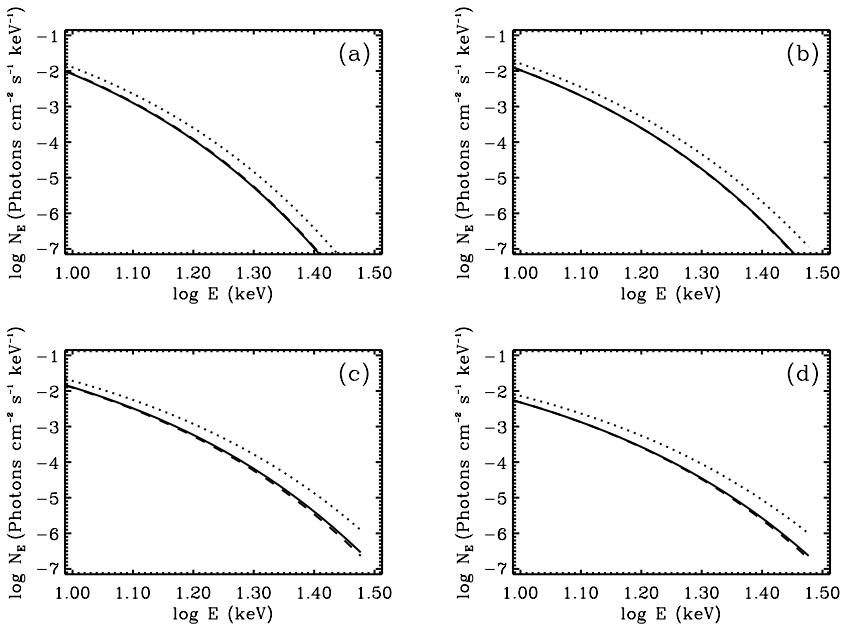

Figure 4. Rotation rate dependence: general relativistic spectra including light-bending effects from an accretion disc around a neutron star. Panel (a) corresponds to $i = 0°$, panel (b) to $i = 30°$, panel (c) to $i = 60°$ and panel (d) to $i = 85°$. In each panel, the solid curve corresponds to $\Omega = 0\,\mathrm{rad\,s^{-1}}$, the adjacent dashed curve corresponds to $\Omega = 7001\,\mathrm{rad\,s^{-1}}$ (the mass-shed limit) and the dotted curve corresponds to $\Omega = 3647\,\mathrm{rad\,s^{-1}}$. The values of all the other parameters are as given in Fig. 1.

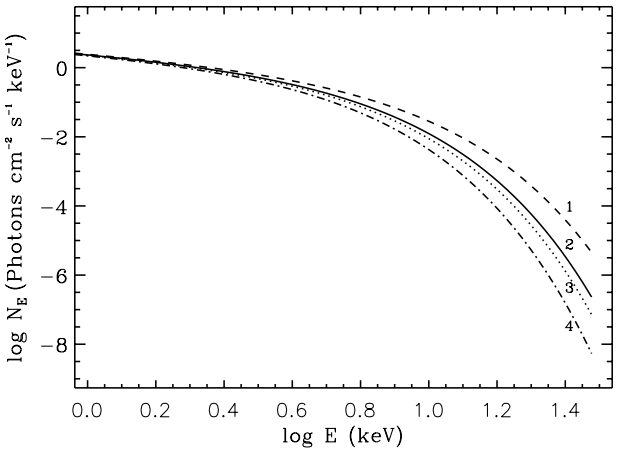

Figure 5. EOS model dependence: general relativistic spectra including light-bending effects from an accretion disc around a neutron star of mass-shed configuration. Curve (1) corresponds to the EOS model (A) ($\Omega = 11\,026\,\mathrm{rad\,s^{-1}}$), curve (2) to the EOS model (B) ($\Omega = 7001\,\mathrm{rad\,s^{-1}}$), curve (3) to the EOS model (C) ($\Omega = 6085\,\mathrm{rad\,s^{-1}}$) and curve (4) to the EOS model (D) ($\Omega = 4652\,\mathrm{rad\,s^{-1}}$). The values of all the other parameters are as given in Fig. 1.

According to Shimura & Takahara (1995), the thin blackbody description of the accretion disc, as adopted in this paper, is valid for $0.1\,\dot{M}_E < \dot{M} < \dot{M}_{Edd}$, where $\dot{M}_E \equiv L_{Edd}/c^2$. Here L_{Edd} is the Eddington luminosity and $\dot{M}_{Edd}$ is the true Eddington accretion rate. For the purpose of demonstration, we have taken three different values of $\dot{M}$ in this range (for the mass-shed configuration) and plotted the corresponding spectra in Fig. 2. As is expected, we see that the high-energy part of the spectrum is more sensitive to the value of $\dot{M}$. It is seen that the spectra for different values of $\dot{M}$ are easily distinguishable.

The inclination angle i is a very important parameter in determining the shape of the spectrum and its overall normalization. In Fig. 3, we have plotted the spectra for four inclination angles, for the mass-shed configuration. We see that the observed flux at low energies is higher for lower values of i. This is due to the projection effect (proportional to $\cos i$). At higher energies (>10 keV), however, this trend is reversed mainly because the Doppler effect becomes important. The most energetic photons largely come from the inner portion of the disc, where the linear speed of accreted matter is comparable to the speed of light. The net effect of Doppler broadening is a net blueshift of the spectrum, as a larger amount of the flux comes from the blueshifted regions than from the redshifted regions. This is a monotonic trend, but it will be noticed from Fig. 3 that the curve for $i = 85°$ overtakes that for $i = 60°$ only at the edge of the figure, i.e. at energies ≥ 30 keV. This is due to the fact that between these two inclinations the difference in the $\cos i$ factor is severe, and the blueshift overcomes this only at high energies.

In Fig. 4, we have four panels for four inclination angles. In each panel, we have shown spectra for three different Ω (corresponding to non-rotating, intermediate and mass-shed configurations). With the increase of Ω, the disc temperature profile does not vary monotonically (see fig. 3a of Bhattacharyya et al. 2000). Hence, the behaviour of the spectrum is also non-monotonic with Ω. For non-rotating and mass-shed configurations (for the assumed values of other parameters) the temperature profiles are very similar. As a result, the plotted spectra for these two cases lie almost on top of each other. However, for $i = 0°$ the flux corresponding to the mass-shed configuration is slightly higher than that for $\Omega = 0$, while the case is opposite at higher inclinations. This is a result of the inclination dependence of the $(1 + z)$ factor given in equation (7).

In Fig. 5, we have compared the spectra for the four EOS models adopted by us, for configurations at the respective mass-shed limits (which correspond to different values of Ω because of the EOS dependence on the stellar structure). The values of all other parameters have been kept the same. We see that the total flux received varies monotonically with the stiffness parameter, and is

higher for the softer EOS. This effect has been noticed earlier by Bhattacharyya et al. (2000). We see that at high energies the fluxes for different EOSs are considerably different. Therefore, fitting the observed spectra of LMXBs with our model spectra, particularly in hard X-rays, may provide a way to constrain the neutron star EOS. Of course it must be remembered that these computations have been made assuming that the magnetic field of the compact object does not limit the inner boundary of the accretion disc. In the presence of sufficiently strong magnetic fields, appropriate modifications must be taken into account while calculating the expected flux at high energies.

5 CONCLUSIONS

In this paper we have computed the observed radiation spectrum from accretion discs around rapidly rotating neutron stars using fully general relativistic disc models. This is the first time such a calculation has been made in an exact way, without making any approximation in the treatment of either rotation or general relativity. In computing the observed spectrum from the disc, we explicitly include the effects of Doppler shift, gravitational redshift and light bending for an appropriate metric describing space–time around rapidly rotating neutron stars. We find that the effect of light bending is most important in the high-energy (>3 keV) part of the observed spectrum. Photons at these high energies originate close to the central star, and hence their trajectories are most affected by the light-bending effect. Depending on the viewing angle, this can enhance the observed flux at ~ 10 keV by as much as 250 per cent compared with that expected, if light-bending effects are neglected.

The calculations presented here deal only with the multicolour blackbody disc. In reality, of course, there will be additional contributions to the observed spectrum from the boundary layer and also possibly from an accretion disc corona, both of which are likely to add a power-law component at high energies (Dove, Wilms & Begelman 1997; Popham & Sunyaev 2001). On the other hand, the spectra presented in Figs 2, 3 and 5 should remain essentially unaffected by boundary layer contributions, as these are for neutron stars rotating near the mass-shed limit for which the boundary layer luminosity will be negligible. For slowly rotating neutron stars, the disc component of the spectrum can be obtained by fitting and removing the contribution of the boundary layer, provided a good model for the boundary layer spectrum is available. Popham & Sunyaev (2001) have calculated the boundary layer spectrum using the Newtonian approximation. General relativistic modifications need to be included in these calculations to get a realistic estimate of the spectrum of the boundary layer. We plan to address this issue in a future work. In the slow-rotation case, the spectrum of the disc itself may be modified by the presence of a boundary layer if it extends beyond the disc inner radius assumed in our computations here, thus curtailing the inner edge of the disc.

In addition to the contributions of the boundary layer, the possible contribution of an accretion disc corona to the emergent spectrum could also be significant. To be able to constrain the EOS models of neutron stars using the observed spectrum, this contribution must also be accurately estimated. In the present work, we restrict ourselves to thin blackbody and non-magnetic accretion discs in order to understand the effect of the EOS models describing neutron stars on the spectrum of the accretion disc alone (and thus neglect the effect of a corona). We view this as the first step in the modelling of spectra of accreting neutron stars, including the effects of general relativity and rotation.

The comparison of the non-rotating limit of our results with those of the fitting routine GRAD in the X-ray spectral reduction package XSPEC (Ebisawa et al. 1991) model shows that the latter overpredicts the high-energy component of the flux by a large factor. With the help of Ebisawa & Hanawa (private communication) we have been able to trace this disagreement to certain simplifying approximations made in the GRAD code, as well as a couple of incorrect expressions being used there. Conclusions based on the use of the GRAD routine may therefore need to be revised in the light of the new calculations presented here.

The computation of the complete spectrum in the manner presented here is time-consuming and is therefore not suited to routine use. Hence, in order to make our results available for routine spectral fitting work, we intend presenting a series of approximate parametric fits to our computed spectra in a forthcoming publication.

The spectra presented here will find use in constraining the combined parameter set of the mass, the rotation speed and possibly the EOS, particularly of weakly magnetized, rapidly rotating neutron stars. The relevant signatures are most prominent in hard X-rays, above ~ 10 keV. Sensitive observations of hard-X-ray spectra of LMXBs, therefore, are needed to utilize fully the potential of these results.

ACKNOWLEDGMENTS

We thank the late Bhaskar Datta for discussions in the early stages of the work. We thank Ranjeev Misra for providing us with the GRAD routine and for many discussions. We are very thankful to K. Ebisawa and T. Hanawa for discussions which helped resolve the discrepancy between our results and those obtained from the GRAD routine. We are also grateful to B. R. Iyer for valuable suggestions during the course of this work. SB thanks Pijush Bhattacharjee for encouragement.

REFERENCES

Asaoka I., 1989, PASJ, 41, 763
Backer D. C., Kulkarni S. R., Heiles C., Davis M. M., Goss W. M., 1982, Nat, 300, 615
Baldo M., Bombaci I., Burgio G. F., 1997, A&A, 328, 274
Bhattacharya D., van den Heuvel E. P. J., 1991, Phys. Rep., 203, 1
Bhattacharyya S., Thampan A. V., Misra R., Datta B., 2000, ApJ, 542, 473
Bhattacharyya S., Misra R., Thampan A. V., 2001, ApJ, 550, 841
Chandrasekhar S., 1983, The Mathematical Theory of Black Holes. Oxford University Press, London
Cook G. B., Shapiro S. L., Teukolsky S. A., 1994, ApJ, 424, 823
Datta B., Thampan A. V., Bombaci I., 1998, A&A, 334, 943
Dove J. B., Wilms J., Begelman M. C., 1997, ApJ, 487, 747
Ebisawa K., Mitsuda K., Hanawa T., 1991, ApJ, 367, 213
Luminet J. P., 1979, A&A, 75, 228
Misner C. W., Thorne K. S., Wheeler A. J., 1973, Gravitation. Freeman, San Francisco
Mitsuda K. et al., 1984, PASJ, 36, 741
Page D. N., Thorne K. S., 1974, ApJ, 191, 499
Pandharipande V. R., 1971, Nucl. Phys., A178, 123
Popham R., Sunyaev R. A., 2001, ApJ, 547, 355
Sahu P. K., Basu R., Datta B., 1993, ApJ, 416, 267
Shimura T., Takahara F., 1995, ApJ, 445, 780
Sun W.-H., Malkan M. A., 1989, ApJ, 346, 68
Sunyaev R. A., Shakura N. I., 1986, Sov. Astron. Lett., 12, 117
Thampan A. V., Datta B., 1998, MNRAS, 297, 570
Van der Klis M., 2000, ARA&A, 38, 717
Walecka J. D., 1974, Ann. Phys., 83, 491
Wijnands R., Van der Klis M., 1998, Nat, 394, 344

APPENDIX A

For convenience, we use μ $(=\cos\theta)$ instead of θ and s $[=\bar{r}/(A+\bar{r})]$ instead of r as the coordinates. Consequently, equation (1) becomes

$$\begin{aligned} \mathrm{d}S^2 = & -\mathrm{e}^{\gamma+\rho}\,\mathrm{d}t^2 + \mathrm{e}^{2\alpha}\{[A^2/(1-s)^4]\,\mathrm{d}s^2 \\ & + A^2[s/(1-s)]^2[1/(1-\mu^2)]\,\mathrm{d}\mu^2\} \\ & + \mathrm{e}^{\gamma-\rho}A^2[s/(1-s)]^2(1-\mu^2)(\mathrm{d}\phi-\omega\,\mathrm{d}t)^2. \end{aligned} \tag{A1}$$

Here, A is a known constant for the dimension of distance.

Now it is straightforward to calculate the geodesic equations for photons, which are given below.

$$\mathrm{d}t/\mathrm{d}\lambda = \mathrm{e}^{-(\gamma+\rho)}(1-\omega L), \tag{A2}$$

$$\mathrm{d}\phi/\mathrm{d}\lambda = \mathrm{e}^{-(\gamma+\rho)}\omega(1-\omega L) + L/\{\mathrm{e}^{\gamma-\rho}A^2[s/(1-s)]^2(1-\mu^2)\}, \tag{A3}$$

$$\begin{aligned} (\mathrm{d}s/\mathrm{d}\lambda)^2 = & \ \mathrm{e}^{-2\alpha}[(1-s)^4/A^2][\![\mathrm{e}^{-(\gamma+\rho)}(1-\omega L)^2 \\ & - L^2/\{\mathrm{e}^{\gamma-\rho}A^2[s/(1-s)]^2(1-\mu^2)\}] \\ & - s^2(1-s)^2[1/(1-\mu^2)]y^2, \end{aligned} \tag{A4}$$

$$\mathrm{d}\mu/\mathrm{d}\lambda = y, \tag{A5}$$

$$\begin{aligned} \mathrm{d}y/\mathrm{d}\lambda = & -2[\![\alpha_{,s} + \{1/[s(1-s)]\}]\!]y(\mathrm{d}s/\mathrm{d}\lambda) \\ & + \alpha_{,\mu}\{1/[s(1-s)]\}^2(1-\mu^2)(\mathrm{d}s/\mathrm{d}\lambda)^2 \\ & - \{\alpha_{,\mu} + [\mu/(1-\mu^2)]\}y^2 \\ & + \{(1/2)\,\mathrm{e}^{\gamma-\rho-2\alpha}(\gamma_{,\mu}-\rho_{,\mu})(1-\mu^2)^2\omega^2 \\ & - \mathrm{e}^{\gamma-\rho-2\alpha}\mu(1-\mu^2)\omega^2 \\ & + \mathrm{e}^{\gamma-\rho-2\alpha}(1-\mu^2)^2\omega\omega_{,\mu} \\ & - (1/2)\,\mathrm{e}^{\gamma+\rho-2\alpha}(\gamma_{,\mu}+\rho_{,\mu})[(1-s)/(As)]^2(1-\mu^2)\} \\ & \times(\mathrm{d}t/\mathrm{d}\lambda)^2 + \mathrm{e}^{\gamma-\rho-2\alpha}(1-\mu^2)^2\{-\omega_{,\mu} - \omega(\gamma_{,\mu}-\rho_{,\mu}) \\ & + 2\omega[\mu/(1-\mu^2)]\}(\mathrm{d}\phi/\mathrm{d}\lambda)(\mathrm{d}t/\mathrm{d}\lambda) \\ & + \mathrm{e}^{\gamma-\rho-2\alpha}(1-\mu^2)^2[(1/2)(\gamma_{,\mu}-\rho_{,\mu}) \\ & - \mu/(1-\mu^2)](\mathrm{d}\phi/\mathrm{d}\lambda)^2, \end{aligned} \tag{A6}$$

where λ is the affine parameter, L is the negative of the ratio of the ϕ-component of the angular momentum and the t-component of the angular momentum of the photon, and a comma followed by a variable as subscript to a quantity represents a derivative of the quantity with respect to the variable.

This paper has been typeset from a TEX/LATEX file prepared by the author.